# On the Mechanism of Formation of Vesicles from Poly(Ethylene Oxide)-*block*-Poly(Caprolactone) Copolymers

Dave J. Adams,[a]* Craig Kitchen,[b] Sarah Adams,[b] Steve Furzeland,[b] Derek Atkins,[b] Peter Schuetz,[b] Christine M. Fernyhough,[c] Nadia Tzokova,[c] Anthony J. Ryan [c] and Michael F. Butler [b]*

*a) Unilever Research Colworth, Sharnbrook, Bedfordshire, MK44 1LQ, current address: Department of Chemistry, University of Liverpool, Crown Street, Liverpool, L69 7ZD, UK; b) Unilever Research Colworth, Sharnbrook, Bedfordshire, MK44 1LQ, UK; c) Department of Chemistry, Dainton Building, The University of Sheffield, Brook Hill, Sheffield, S3 7HF, UK*

Email: Michael.Butler@Unilever.com; d.j.adams@liverpool.ac.uk

SUPPORTING INFORMATION

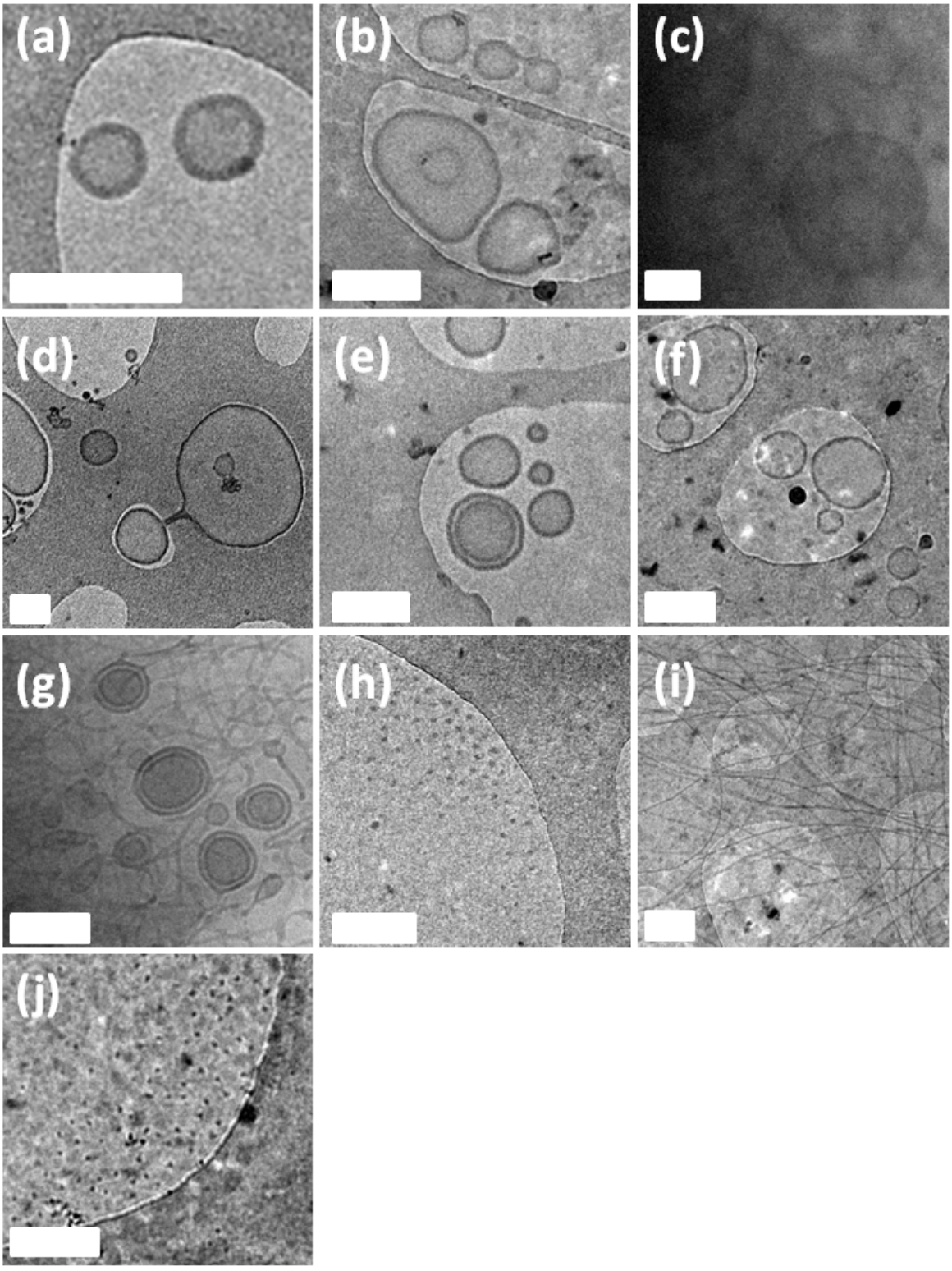


**Figure S1.** Representative cryo-TEM images of PEO-b-PCL samples in 20 % THF for which self-assembled structures were obtained. (a) $PEO_{16}$-*b*-$PCL_{49}$, (b) $PEO_{16}$-*b*-$PCL_{38}$, (c) $PEO_{45}$-*b*-$PCL_{101}$, d) $PEO_{23}$-*b*-$PCL_{47}$, (e) $PEO_{23}$-*b*-$PCL_{40}$ (no structures observed) (f) $PEO_{16}$-*b*-$PCL_{23}$

(no structures observed) (g) $PEO_{23}$-*b*-$PCL_{28}$, (h) $PEO_{45}$-*b*-$PCL_{43}$, (i) $PEO_{16}$-*b*-$PCL_{14}$, (j) $PEO_{113}$-*b*-$PCL_{56}$. The scale bar in all cases represents 200nm.

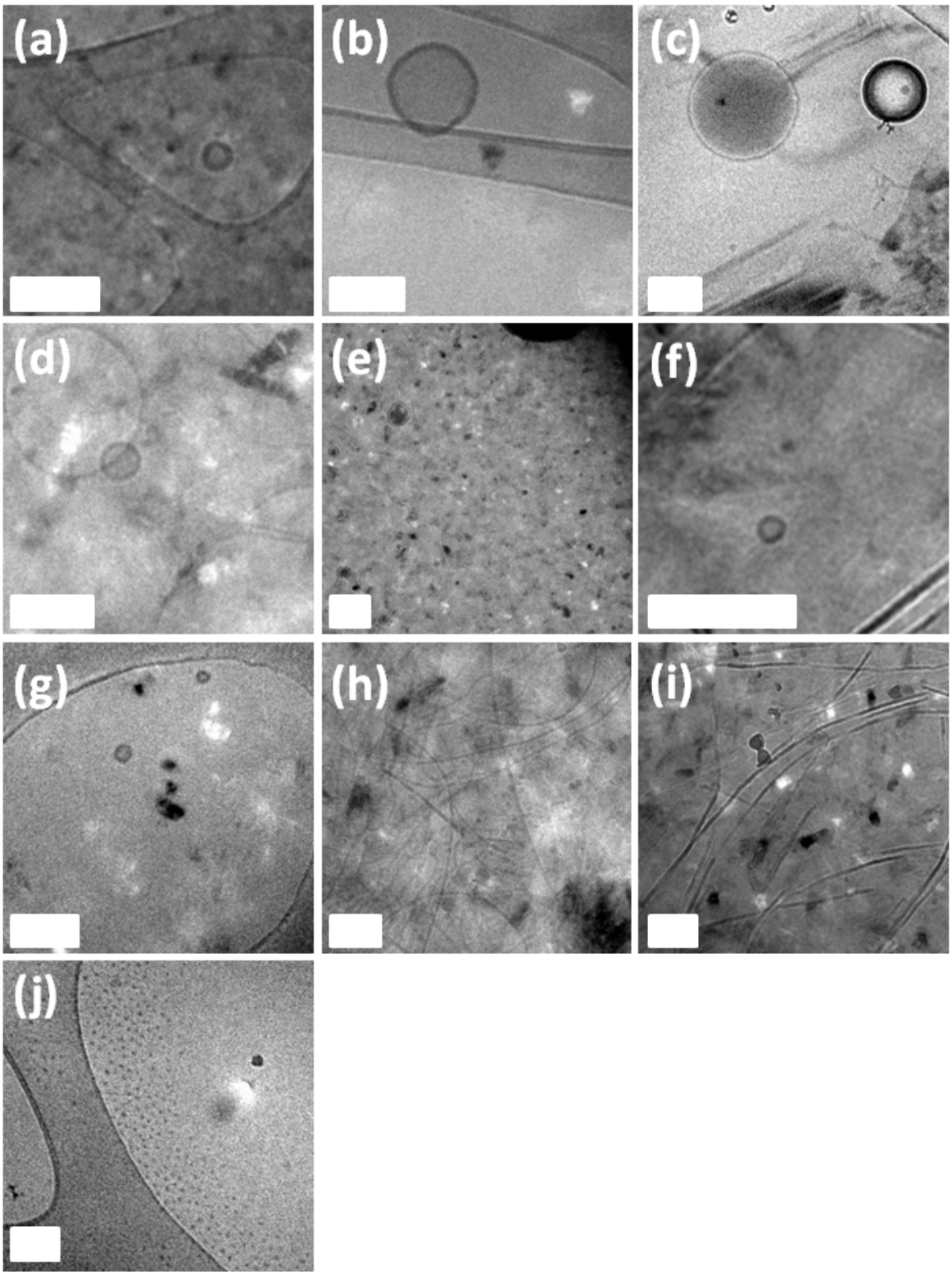


**Figure S2.** Representative cryo-TEM images of dialysed PEO-b-PCL samples, for which self-assembled structures were obtained. (a) $PEO_{16}$-*b*-$PCL_{49}$, (b) $PEO_{16}$-*b*-$PCL_{38}$, (c) $PEO_{45}$-

*b*-$PCL_{101}$, d) $PEO_{23}$-*b*-$PCL_{47}$, (e) $PEO_{23}$-*b*-$PCL_{40}$ (no structures observed) (f) $PEO_{16}$-*b*-$PCL_{23}$ (almost no structures observed) (g) $PEO_{23}$-*b*-$PCL_{28}$, (h) $PEO_{45}$-*b*-$PCL_{43}$, (i) $PEO_{16}$-*b*-$PCL_{14}$, (j) $PEO_{113}$-*b*-$PCL_{56}$. The scale bar in all cases represents 200nm.

**Figure S3** shows the influence of THF content on the size of the vesicles for $PEO_{23}$-*b*-$PCL_{28}$, along with the effect of rate of water addition on the final vesicle size. For the range of rates used (0.005 to 8 mL $min^{-1}$), the final vesicle size was constant for dialysed and non-dialysed samples.

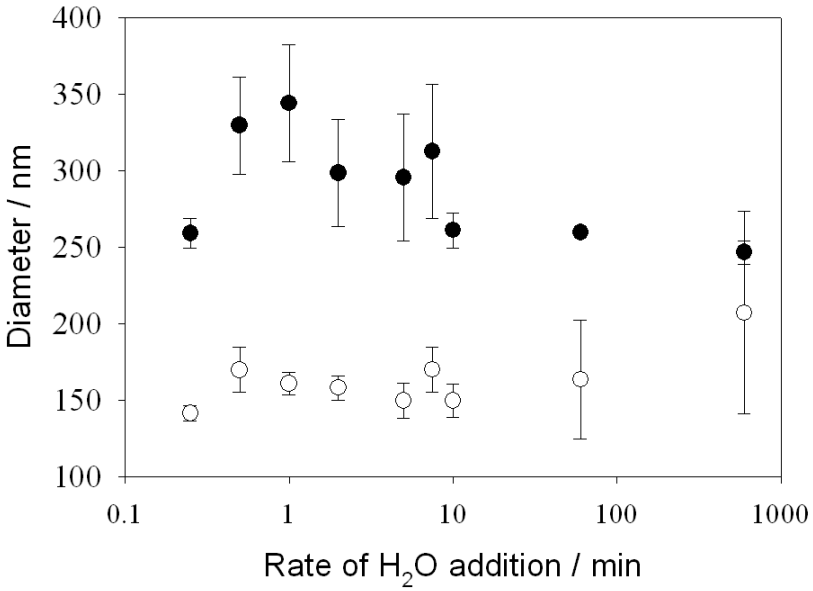


**Figure S3.** Variation in z-average diameter with rate of water addition to a solution of $PEO_{23}$-*b*-$PCL_{28}$ in THF (initial concentration 10 mg $mL^{-1}$, final concentration 2 mg $mL^{-1}$); ●, before dialysis and ○, after dialysis. The error bars were calculated from the variation in diameter from at least five different samples.

Extrusion had a significant effect on the polydispersity of the structures observed by cryo-TEM and DLS. **Figure S4** shows correlograms of the vesicle-forming sample ($PEO_{23}$-*b*-$PCL_{40}$) before and after extrusion through the 100nm polycarbonate membrane demonstrating the measurable effect of extrusion on decreasing the polydispersity of aggregate sizes.

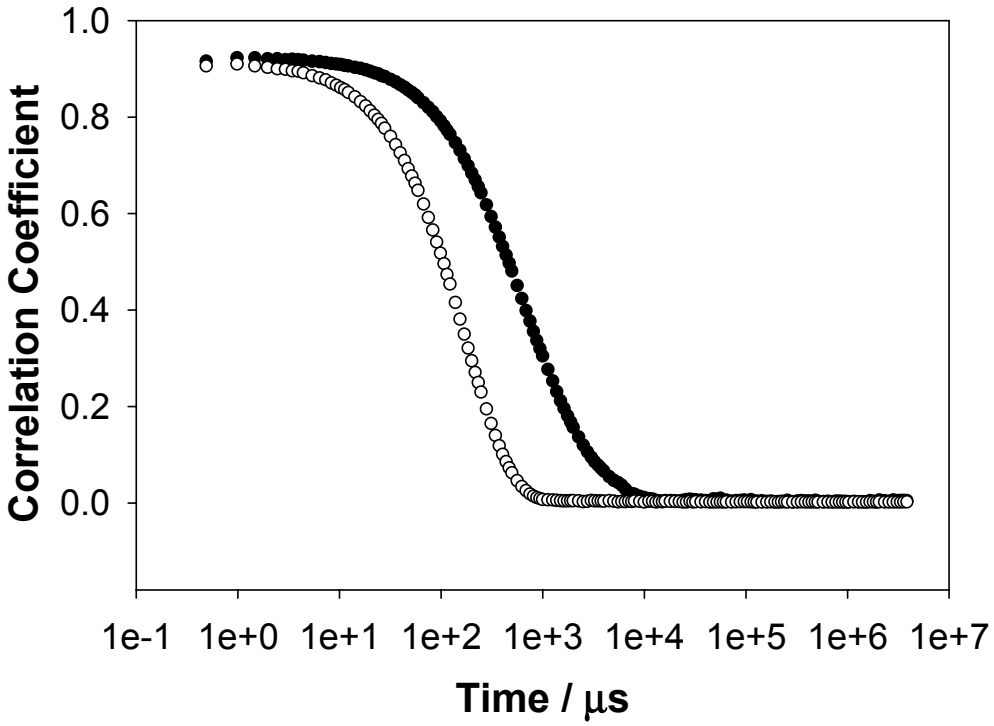


**Figure S4.** Example correlogram obtained by DLS (●) before and (○) after extrusion of a $PEO_{23}$-*b*-$PCL_{40}$ solution through a 100 nm membrane.

Zimm plots for the extruded vesicle samples are shown in Figure S5.

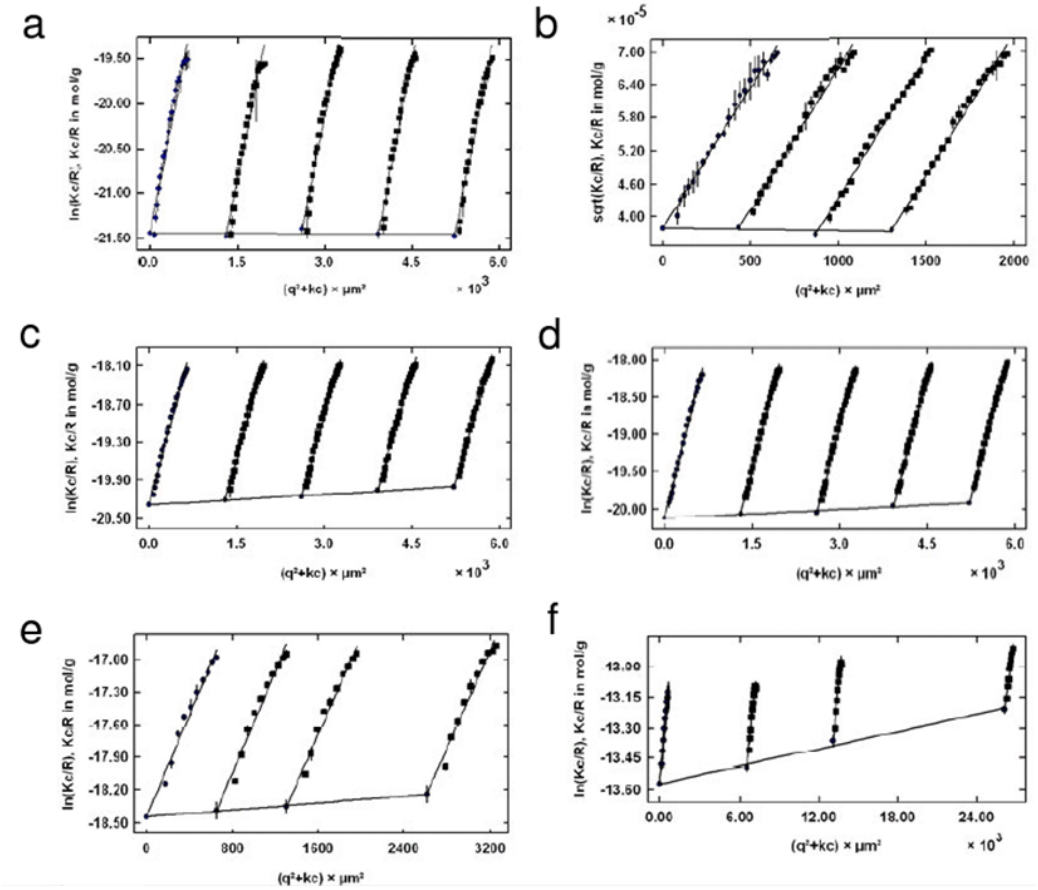


**Figure S5.** Zimm plots for the vesicle-forming systems, after dialysis and extrusion: (a) $PEO_{23}$-*b*-$PEO_{16}$, (b) $PEO_{45}$-*b*-$PCL_{101}$, (c) $PEO_{23}$-*b*-$PCL_{47}$, (d) $PEO_{23}$-*b*-$PCL_{40}$, (e) $PEO_{23}$-*b*-$PCL_{28}$, (f) $PEO_{45}$-*b*-$PCL_{43}$.

**Figure S6** shows an example SAXS pattern (two repeats of fresh batches of extruded vesicle solution), from which the vesicle membrane thickness was measured.

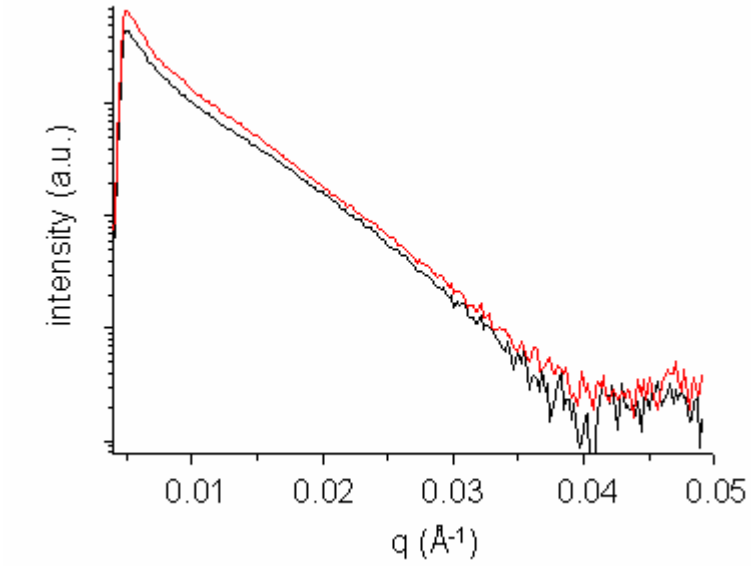


**Figure S6.** Example SAXS patterns for two freshly prepared extruded and dialysed $PEO_{23}$-*b*-$PCL_{40}$ samples, showing the minimum around $0.04Å^{-1}$ resulting from the membrane thickness.